SUPPORTING INFORMATION

Aromatic-aromatic interactions and hydrogen bonding in amino acid based ionic liquids

Wenbo Dong,[a] Patrick R. Batista,[a,b] Jan Blasius[a], Barbara Kirchner[a*]
[a]Mulliken Center for Theoretical Chemistry, University of Bonn, Beringstr. 4+6, D-53115 Bonn, Germany
[b]Institute of Chemistry, University of Campinas, Monteiro Lobato, 270, Cidade Universitária, 13083-862, Campinas, São Paulo, Brazil
*email:kirchner@thch.uni-bonn.de
January 16, 2025

S1 Electrostatic Potential Surface and CHELPG Atomic Charges

S1.1 Static Quantum Chemical Calculations

Quantum chemical calculations were carried out in order to obtain the electrostatic potentials (ESPs) of the amino acid anions. Therefore, geometry optimizations and frequency calculations were performed with the Orca[1] software package employing the PBEh-3c[2] composite method, which was paired with a modified def2-SV(P) basis set, termed as def2-mSVP. This level of theory includes the DFT-D3 dispersion correction scheme[3,4] and a geometrical counterpoise correction[2,5] in order to account for the intermolecular and intramolecular interactions and basis set superposition error, respectively. The grid level was chosen as 5 and a tight convergence criteria was selected for the SCF energy calculations, as well as in geometry optimizations.

S1.2 Results and Discussion

Before assessing the bulk phase structure of the different ILs, the chemical properties of the individual amino acid anions will be investigated. To achieve this, the gas phase ESPs were mapped onto the electron density as shown in Figure S1. Thus, the negative charge carried by the anions is located at the deprotonated carboxylic acid group, which makes it prone to acting as hydrogen bond acceptor. Another common feature among the amino acid anions can be observed around the amine group, where the nitrogen atom exhibits an electron excess induced by its lone pair, while the hydrogen atoms show an electron deficit, thus potentially acting as hydrogen bond donor sites. One exception regarding this observation is proline, since the amine group is enclosed in the heterocycle. Although an electron excess and deficit can still be observed at the nitrogen and hydrogen atom, respectively, the charge separation is less pronounced as compared to the other amino acid anions.
When comparing the various amino acid residues, significant differences can be observed in the electron density distribution. The terminal methyl group of $[ala]^-$ is only slightly polarized, with some electron excess and deficit around the carbon and hydrogen atoms, respectively. Therefore, this methyl group is predominantly non-polar and prone for hydrophilic interactions. $[pro]^-$, the only amino acid anion which features a non-aromatic ring, shows a dispersed distribution of the electron density around its pyrrolidine heterocycle.

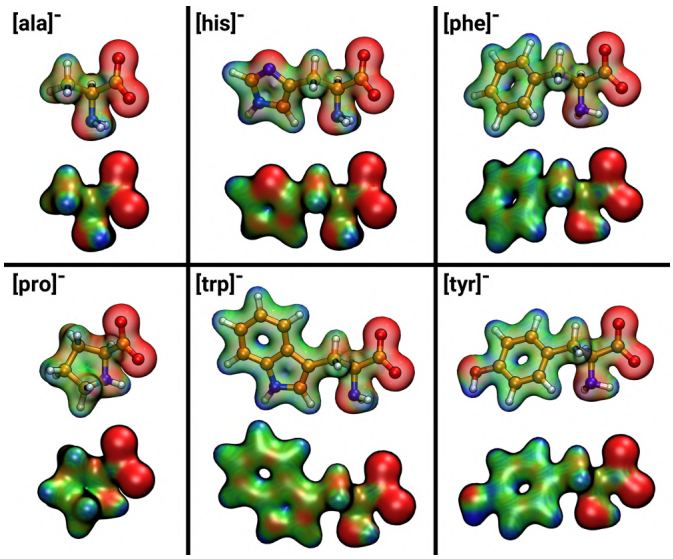

Figure S1: Gas phase electrostatic potentials of the amino acid anions mapped onto the electron density (isosurface value 0.04). The color scale is chosen from -0.1 (blue) to 0.1 (red).

The four aromatic amino acid anions display contrasting electron density distributions around their ring structures, resulting in probable differences with respect to the chemical behaviour. In the case of $[his]^-$ and $[trp]^-$, the two aromatic amino acids featuring heterocycles, the area around the nitrogen atoms exhibits a pronounced negative charge. These can also be supported by CHELPG atomic charges data. Overall, the nitrogen atoms within the ring lowers the π-electron density and thus the aromaticity. Many studies have attempted to gain insight into the aromaticity of a particular heterocycle by comparing its bond lengths with those of related molecules.[6] The Bird index can be easily derived from experimentally determined bond lengths. The utility of this index is reflected in its application to five-membered heterocycles and their mesoionic derivatives. This is also reflected by the Bird indexes of imidazole and indole, which are calculated as 64[6] and 70[7], respectively. For comparison, the Bird index of benzene equals to 100[8] and is chosen as reference. Bird indices smaller than 100 indicate a decreased aromaticity as compared to benzene. Additionally, both anions show a slight negative charge between the C-C bonds within the rings which most likely occurs due to the partial double bond character of the aromatic C-C bonds. The same is observed for $[phe]^-$ and $[tyr]^-$, inasmuch as the C-C bonds within the rings show a slight increase in the electron density. Among the six amino acid anions discussed, $[tyr]^-$ is the only one containing a hydroxyl group. From the electrostatic potential plots, it becomes evident that the hydroxyl oxygen and hydrogen atoms show a pronounced bond donor and acceptor characteristics, respectively. Thus, this additional hydrogen bond interaction site may affect the bulk phase structure significantly.
The CHELPG atomic charges for each atom of the cation and anions are listed in Tables S1–S7, along with the corresponding atom numbers in Figures S2–S8. In the case of anions, the amine nitrogen atoms of the anions always shows the most negative number, even above 1 (except $[pro]^-$, the amine in [pro] is a secondary one). Besides, the carboxylate group carbons and the carbons linked to the nitrogen atoms give more positive data. A significant increase in the electron density can be observed around the ring carbon atom attached to the carboxylate group compared to the other ring carbon atoms. While the hydrogen atoms show decreased electron density, some electron excess is located around the C-C bonds. A significant increase in the electron density can be observed around the ring carbon atom attached to the carboxylate group compared to the other ring carbon atoms in $[C_2C_1im][his]$ and $[C_2C_1im][phe]$.

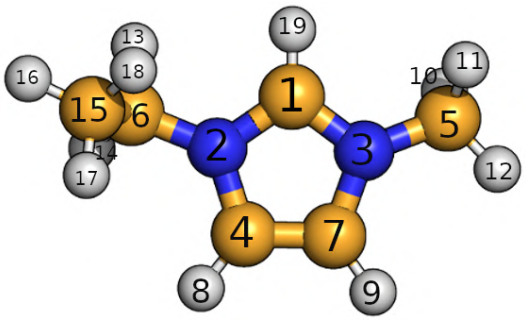

Figure S2: Atomic number of $[C_2C_1im]^+$.

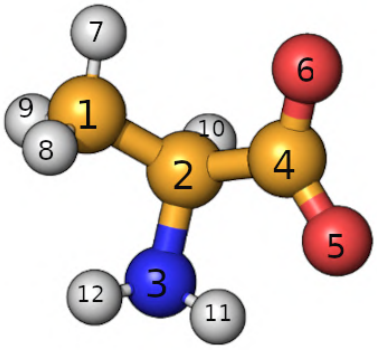

Figure S3: Atomic number of $[ala]^-$.

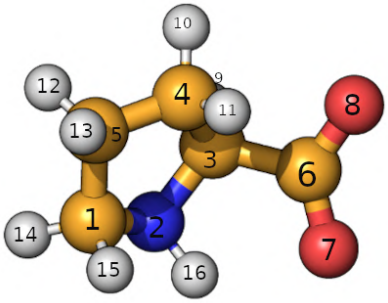

Figure S4: Atomic number of $[pro]^-$.

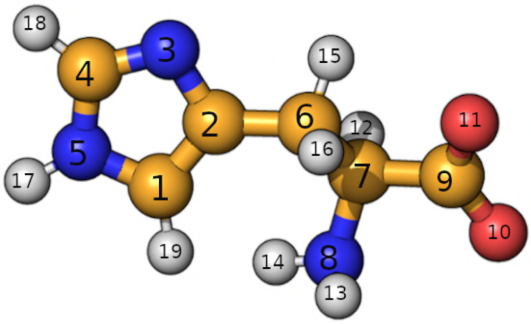

Figure S5: Atomic number of $[his]^-$.

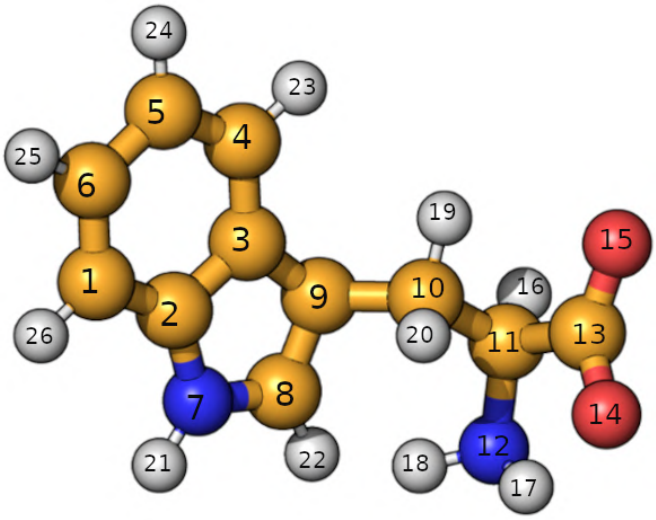

Figure S6: Atomic number of $[trp]^-$.

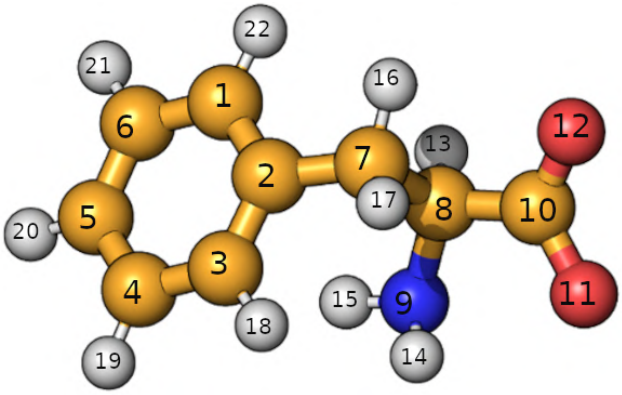

Figure S7: Atomic number of $[phe]^-$.

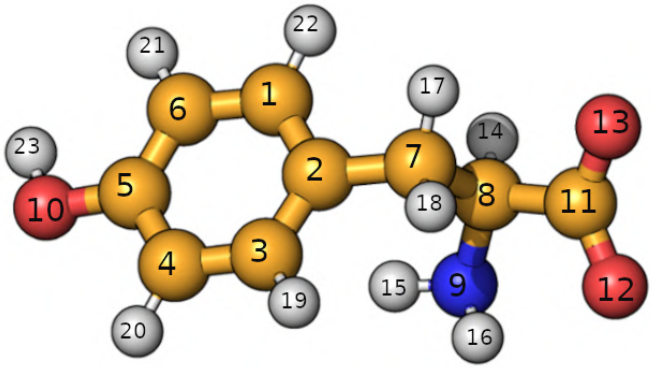

Figure S8: Atomic number of $[tyr]^-$.

Table S1: Partial CHELPG atomic charges of $[C_2C_1im]^+$.

Atomic Number	Atom	Charge
1	C	-0.13
2	N	0.09
3	N	0.31
4	C	-0.21
5	C	-0.44
6	C	0.08
7	C	-0.26
8	H	0.26
9	H	0.26
10	H	0.20
11	H	0.19
12	H	0.19
13	H	0.07
14	H	0.08
15	C	-0.23
16	H	0.11
17	H	0.09
18	H	0.09
19	H	0.25

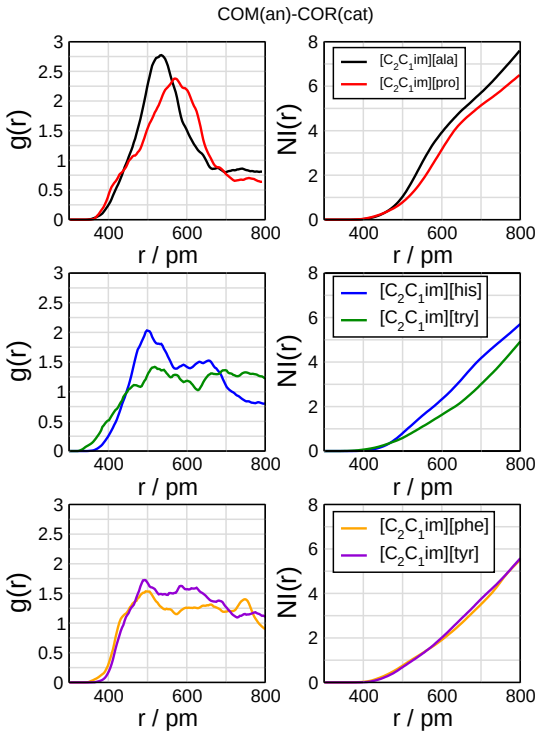

Figure S9: Radial pair distribution functions and number integrals between the center of mass of the anion and the center of ring of the cation. an: anion; cat: cation.

Table S2: Partial CHELPG atomic charges of $[ala]^-$.

Atomic Number	Atom	Charge
1	C	-0.40
2	C	0.66
3	N	-1.03
4	C	0.62
5	O	-0.78
6	O	-0.8
7	H	0.06
8	H	0.10
9	H	0.04
10	H	-0.11
11	H	0.30
12	H	0.33

Table S3: Partial CHELPG atomic charges of $[pro]^-$.

Atomic Number	Atom	Charge
1	C	0.32
2	N	-0.83
3	C	0.25
4	C	0.09
5	C	-0.19
6	C	0.82
7	O	-0.81
8	O	-0.86
9	H	-0.03
10	H	-0.05
11	H	0.01
12	H	0.05
13	H	-0.01
14	H	-0.05
15	H	-0.03
16	H	0.33

Table S4: Partial CHELPG atomic charges of $[his]^{-}$.

Atomic Number	Atom	Charge
1	C	-0.24
2	C	0.46
3	N	-0.63
4	C	0.20
5	N	-0.43
6	C	-0.33
7	C	0.43
8	N	-1.03
9	C	0.71
10	O	-0.79
11	O	-0.81
12	H	-0.05
13	H	0.33
14	H	0.35
15	H	0.11
16	H	0.10
17	H	0.34
18	H	0.11
19	H	0.18

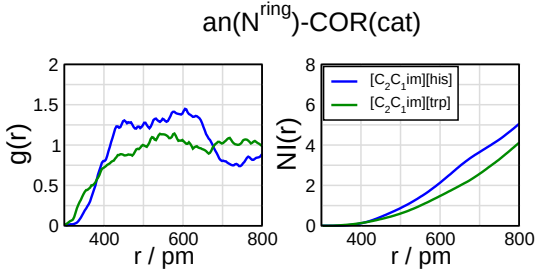

Figure S10: Radial pair distribution functions and number integrals between the ring nitrogen atom of [his] and [trp] which feature a hydrogen atom and the center of ring of the cation.

Table S5: Partial CHELPG atomic charges of $[trp]^{-}$.

Atomic Number	Atom	Charge
1	C	-0.40
2	C	0.33
3	C	0.15
4	C	-0.25
5	C	-0.24
6	C	-0.13
7	N	-0.58
8	C	0.02
9	C	-0.24
10	C	-0.06
11	C	0.47
12	N	-0.96
13	C	0.64
14	O	-0.77
15	O	-0.80
16	H	-0.06
17	H	0.30
18	H	0.32
19	H	0.04
20	H	0.06
21	H	0.37
22	H	0.14
23	H	0.19
24	H	0.14
25	H	0.13
26	H	0.17

Table S6: Partial CHELPG atomic charges of $[phe]^-$.

Atomic Number	Atom	Charge
1	C	-0.15
2	C	0.10
3	C	-0.14
4	C	-0.17
5	C	-0.18
6	C	-0.19
7	C	-0.20
8	C	0.65
9	N	-0.96
10	C	0.59
11	O	-0.75
12	O	-0.77
13	H	-0.13
14	H	0.30
15	H	0.30
16	H	0.03
17	H	0.06
18	H	0.11
19	H	0.13
20	H	0.12
21	H	0.13
22	H	0.13

Table S7: Partial CHELPG atomic charges of $[tyr]^-$.

Atomic Number	Atom	Charge
1	C	-0.10
2	C	-0.08
3	C	0.05
4	C	-0.55
5	C	0.53
6	C	-0.40
7	C	-0.10
8	C	0.62
9	N	-0.98
10	O	-0.65
11	C	0.59
12	O	-0.75
13	O	-0.78
14	H	-0.11
15	H	0.30
16	H	0.31
17	H	0.02
18	H	0.04
19	H	0.10
20	H	0.19
21	H	0.20
22	H	0.14
23	H	0.41

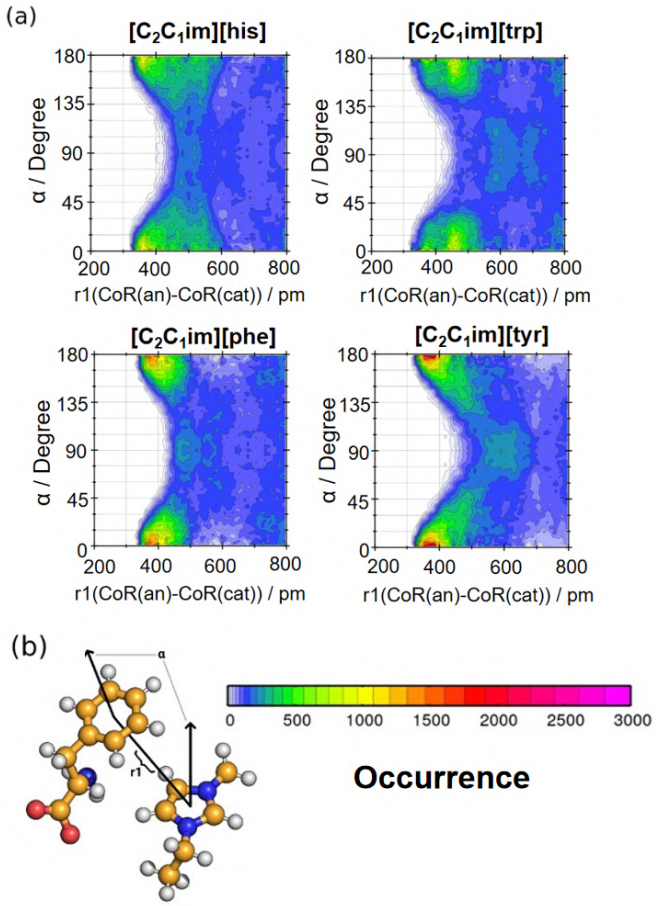

Figure S11: (a) Combined distribution functions correlating the distance between the center of ring of the anion and the center of ring of the cation with the angle between the ring normal vectors of cation and anion. (b) A representation of the interaction in a ball-and-stick model.

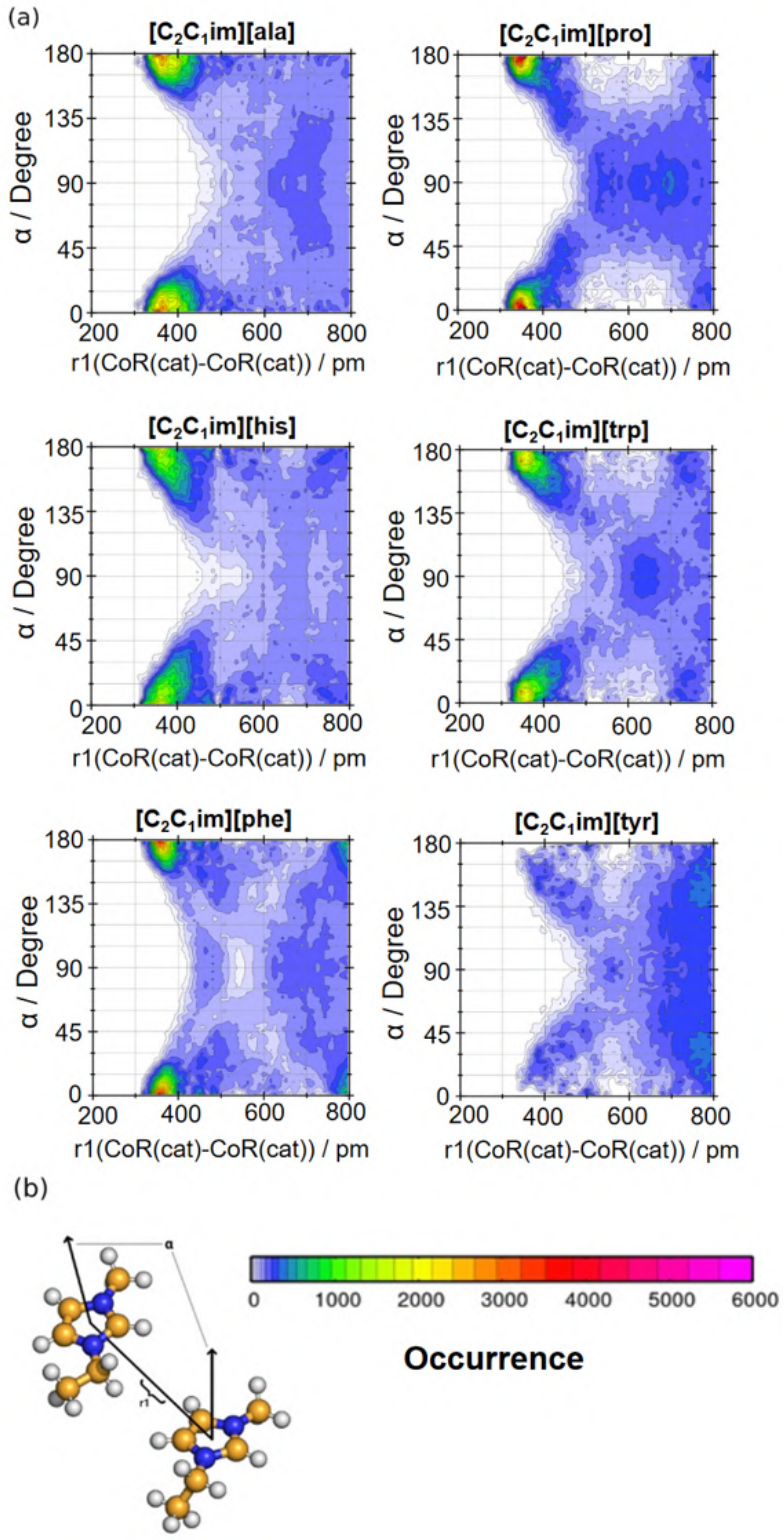

Figure S12: (a) Combined distribution functions correlating the distance between the centers of ring of two cations with the angle between the ring normal vectors of both cations. (b) A representation of the interaction in a ball-and-stick model.

Table S8: The r range values, maximum distances, the g(r) values and the integral number on the g(r)max of the first peaks of the first peaks from the radial distribution functions for four kinds of HB: i) between the carboxylate group oxygen atoms of the anion and the ring hydrogen atoms of the cation; ii) between the amine group nitrogen atom of the anion and the ring hydrogen atoms of the cation; iii) between the carboxylate group oxygen atoms of the anion and the amine group hydrogen atoms of the anion; iv) between the ring hydrogen atoms of the cation and the ring nitrogen atom of $[his]^-$ which does not feature a hydrogen atom.

ion pair	range/pm,(rmax, g(r)max/pm),[NI]			
	an(O^{CO_2})-cat(H^{ring})	an(N^{NH_2})-cat(H^{ring})	an(O^{CO_2})-cat(H^{NH_2})	an(N^{ring})-cat(H^{ring})
$[C_2C_1im][ala]$	160< *r* <300(205, 2.9),[0.4]	170< *r* <280 (228, 1.0),[0.2]	160< *r* <280(215, 1.0),[0.1]	
$[C_2C_1im][pro]$	160< *r* <300(205, 3.9),[0.5]			
$[C_2C_1im][his]$	160< *r* <300(208, 3.2),[0.3]			170< *r* <350(232, 1.25),[0.1]
$[C_2C_1im][trp]$	160< *r* <300(198, 3.2),[0.3]	170< *r* <260(228, 1.2),[0.2]	160< *r* <280(208, 1.1),[0.1]	
$[C_2C_1im][phe]$	160< *r* <300(208, 3.7),[0.3]	170< *r* <260(238, 1.2),[0.2]	160< *r* <280(218, 0.9),[0.1]	
$[C_2C_1im][tyr]$	160< *r* <300(222, 2.0),[0.2]	170< *r* <300(228, 1.3),[0.3]	160< *r* <300(218, 0.8),[0.1]	

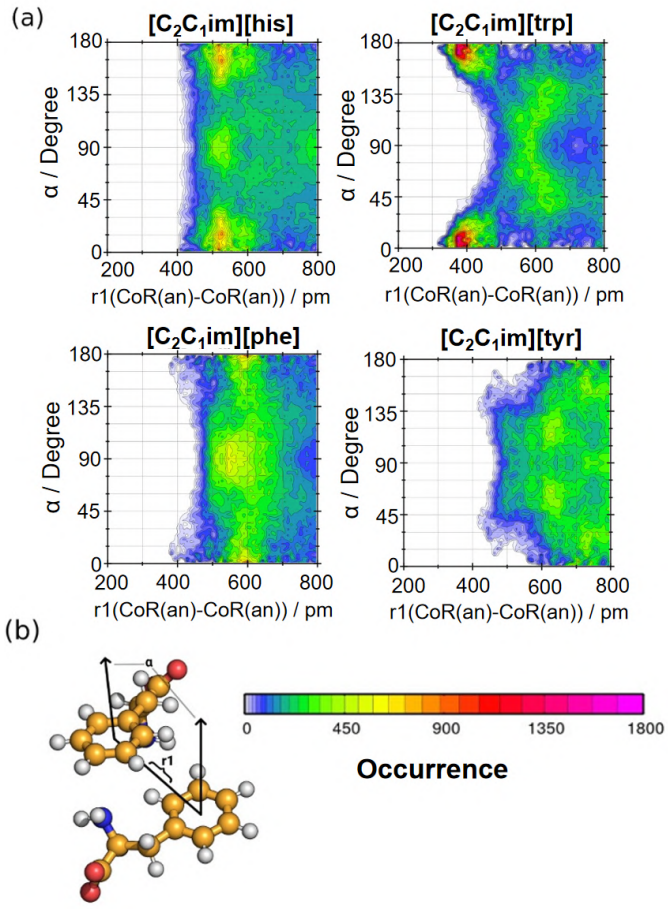

Figure S13: (a) Combined distribution functions correlating the distance between the centers of ring of two anions with the angle between the ring normal vectors of both anions. (b) A representation of the interaction in a ball-and-stick model.

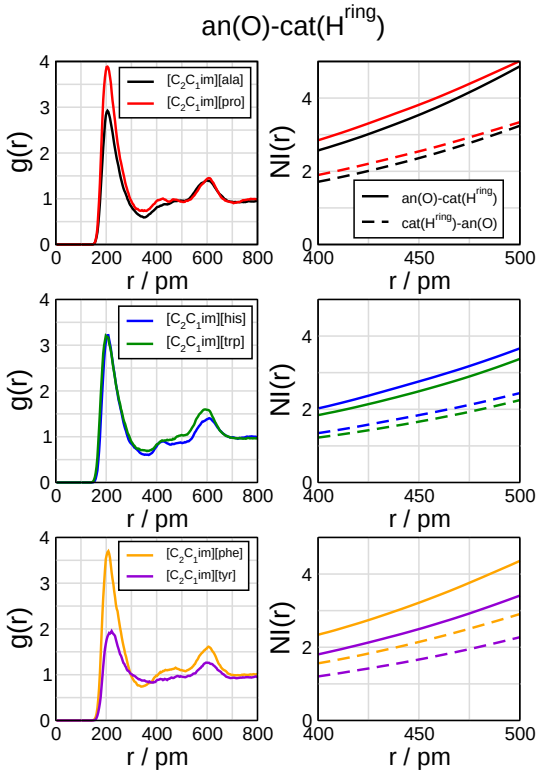

Figure S14: Radial pair distribution functions and number integrals between the carboxylate group oxygen atoms of the anion and the ring hydrogen atoms of the cation.

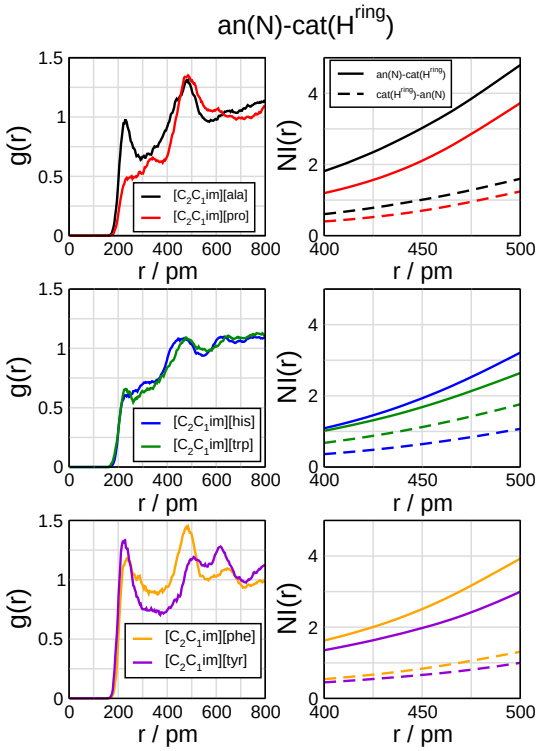

Figure S15: Radial pair distribution functions and number integrals between the amine group nitrogen atom of the anion and the ring hydrogen atoms of the cation.

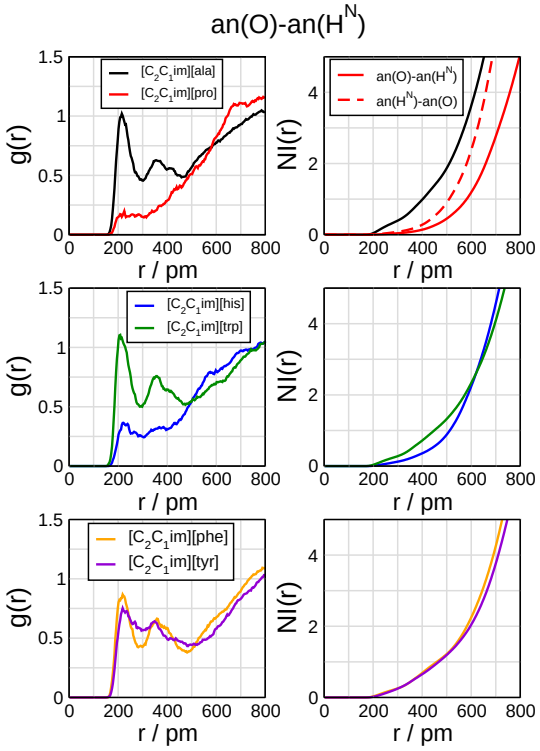

Figure S16: Radial pair distribution functions and number integrals between the carboxylate group oxygen atoms of the anion and the amine group hydrogen atoms of the anion.

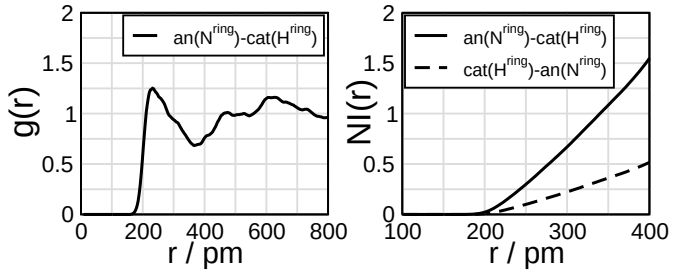

Figure S17: Radial pair distribution functions and number integrals between the ring hydrogen atoms of the cation and the ring nitrogen atom of $[his]^-$ which does not feature a hydrogen atom.

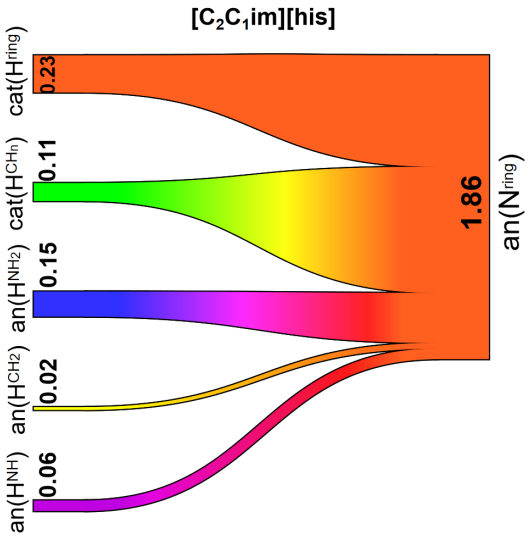

Figure S18: Linear Sankey diagram showing the hydrogen bond topology for $[C_2C_1im][his]$. The labels in the diagram correspond to the following HB donor and acceptor sites: cat(H^{ring}) are the hydrogen atoms in the $[C_2C_1im]^+$ ring; cat(H^{CHn}) are the hydrogen atoms in the CHn groups of the $[C_2C_1im]^+$; an(H^{NH2}) are the hydrogen atoms in NH_2 group of [his]; an(H^{CH2}) are the hydrogen atoms in the chain of the [his]; an(H^{NH}) is the hydrogen atom in NH group of the [his] ring and an(N^{ring}) is the nitrogen atom on the [his] ring without hydrogen.

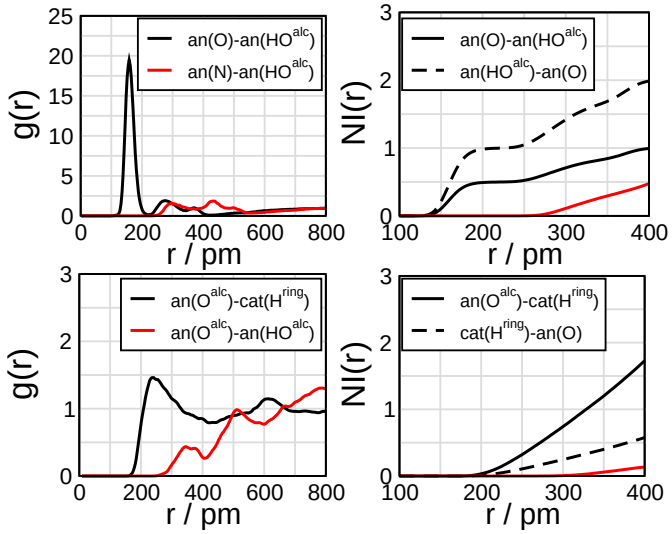

Figure S19: Radial pair distribution functions and number integrals between the carboxylate group oxygen atoms and the hydrogen atom of the alcohol group of the $[tyr]^-$ anion (top); between the amine group nitrogen atom and the hydrogen atom of the alcohol group of the $[tyr]^-$ anion (top); between the alcohol group oxygen atom of the $[tyr]^-$ anion and the ring hydrogen atoms of the cation (bottom); between the alcohol group oxygen atom and the alcohol group hydrogen atom of the $[tyr]^-$

References

(1) Neese, F. The ORCA program system. *WIREs Comp. Mol. Sci.* **2012**, *2*, 73–78.

(2) Grimme, S.; Brandenburg, J. G.; Bannwarth, C.; Hansen, A. Consistent structures and interactions by density functional theory with small atomic orbital basis sets. *J. Chem. Phys.* **2015**, *143*, 054107.

(3) Grimme, S.; Antony, J.; Ehrlich, S.; Krieg, H. A consistent and accurate ab initio parametrization of density functional dispersion correction (DFT-D) for the 94 elements H-Pu. *J. Chem. Phys.* **2010**, *132*, 154104.

(4) Grimme, S.; Ehrlich, S.; Goerigk, L. Effect of the damping function in dispersion corrected density functional theory. *J. Comput. Chem.* **2011**, *32*, 1456–1465.

(5) Kruse, H.; Grimme, S. A geometrical correction for the inter-and intra-molecular basis set superposition error in Hartree-Fock and density functional theory calculations for large systems. *J. Chem. Phys.* **2012**, *136*, 04B613.

(6) Bird, C. A new aromaticity index and its application to five-membered ring heterocycles. *Tetrahedron* **1985**, *41*, 1409–1414.

(7) Bird, C. The application of a new aromaticity index to some bicyclic heterocycles. *Tetrahedron* **1987**, *43*, 4725–4730.

(8) Bird, C. The application of a new aromaticity index to six-membered ring heterocycles. *Tetrahedron* **1986**, *42*, 89–92.